

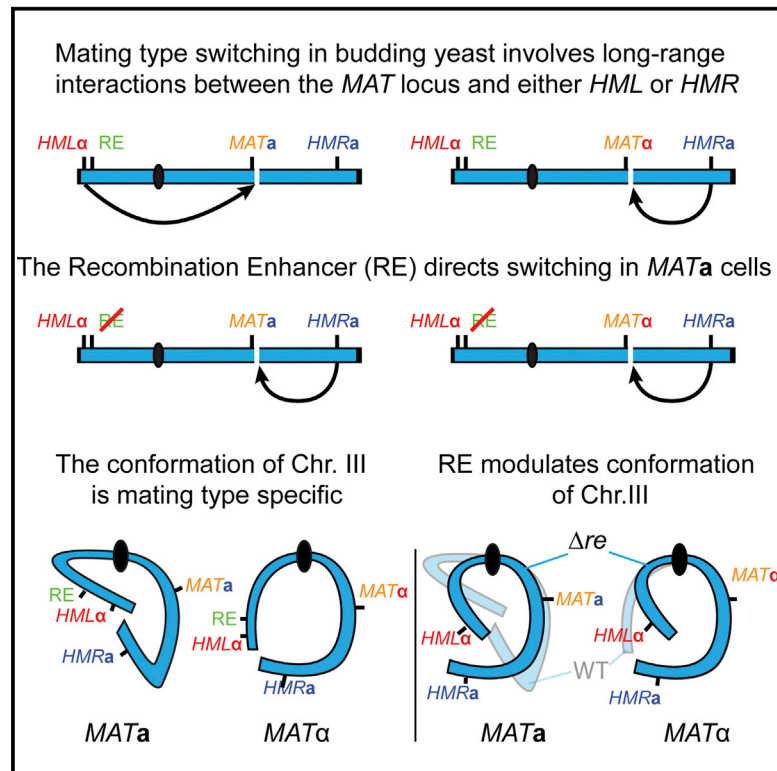
eScholarship@UMassChan

The Conformation of Yeast Chromosome III Is Mating Type Dependent and Controlled by the Recombination Enhancer

Item Type	Journal Article
Authors	Belton, Jon-Matthew;Lajoie, Bryan R.;Audibert, Sylvain;Cantaloube, Sylvain;Lassadi, Imen;Goiffon, Isabelle;Bau, Davide;Marti-Renom, Marc A.;Bystricky, Kerstin;Dekker, Job
Citation	Cell Rep. 2015 Dec 1;13(9):1855-67. doi: 10.1016/j.celrep.2015.10.063. Epub 2015 Nov 19.Link to article on publisher's site
DOI	10.1016/j.celrep.2015.10.063
Rights	<p>This is an open access article under the CC BY-NC-ND license (http://creativecommons.org/licenses/by-nc-nd/4.0/).</p>
Download date	2026-05-08 08:22:45
Item License	http://creativecommons.org/licenses/by-nc-nd/4.0/
Link to Item	https://hdl.handle.net/20.500.14038/39850

The Conformation of Yeast Chromosome III Is Mating Type Dependent and Controlled by the Recombination Enhancer

Graphical Abstract



Highlights

- The conformation of the left arm of yeast chromosome III is mating type specific
- In *MAT_a* cells, *HML_α* is closer to the centromere and the *MAT* locus
- The recombination enhancer is a functionally composite element
- The right half of the RE is a cell-type-specific architectural element

Authors

Jon-Matthew Belton, Bryan R. Lajoie, Sylvain Audibert, ..., Marc A. Marti-Renom, Kerstin Bystricky, Job Dekker

Correspondence

job.dekker@umassmed.edu

In Brief

Yeast mating-type switching involves a mating-type-dependent selection of either the left (*HML*) or right silent mating-type locus (*HMR*) on chromosome III for gene conversion with the active *MAT* locus. One hypothesis has been that this involves differential folding of the chromosome. Belton et al. now show that a 1-kb *cis*-element located within the larger recombination enhancer determines mating-type-dependent chromosome folding so that in *MAT_a* cells *HML* associates with the centromere and *MAT* locus more frequently than in *MAT_α* cells.

Accession Numbers

GSE73890



The Conformation of Yeast Chromosome III Is Mating Type Dependent and Controlled by the Recombination Enhancer

Jon-Matthew Belton,¹ Bryan R. Lajoie,¹ Sylvain Audibert,^{2,3} Sylvain Cantaloube,^{2,3} Imen Lassadi,^{2,3} Isabelle Goiffon,^{2,3} Davide Baù,^{4,5} Marc A. Marti-Renom,^{4,5,6} Kerstin Bystricky,^{2,3} and Job Dekker^{7,*}

¹Program in Systems Biology, Department of Biochemistry and Molecular Pharmacology, University of Massachusetts Medical School, Worcester, MA 01605, USA

²University of Toulouse, UPS, 31062 Toulouse, France

³Laboratoire de Biologie Moléculaire Eucaryote, CNRS, LBME, 31062 Toulouse, France

⁴CNAG-CRG, Centre for Genomic Regulation (CRG), Barcelona Institute of Science and Technology (BIST), Baldiri i Reixac 4, 08028 Barcelona, Spain

⁵Universitat Pompeu Fabra (UPF), Plaça de la Mercè, 10-12, 08002 Barcelona, Spain

⁶Institució Catalana de Recerca i Estudis Avançats (ICREA), Barcelona 08010, Spain

⁷Howard Hughes Medical Institute, Program in Systems Biology, Department of Biochemistry and Molecular Pharmacology, University of Massachusetts Medical School, Worcester, MA 01605, USA

*Correspondence: job.dekker@umassmed.edu

<http://dx.doi.org/10.1016/j.celrep.2015.10.063>

This is an open access article under the CC BY-NC-ND license (<http://creativecommons.org/licenses/by-nc-nd/4.0/>).

SUMMARY

Mating-type switching in yeast occurs through gene conversion between the *MAT* locus and one of two silent loci (*HML* or *HMR*) on opposite ends of the chromosome. *MAT_a* cells choose *HML* as template, whereas *MAT_α* cells use *HMR*. The recombination enhancer (RE) located on the left arm regulates this process. One long-standing hypothesis is that switching is guided by mating-type-specific and possibly RE-dependent chromosome folding. Here, we use Hi-C, 5C, and live-cell imaging to characterize the conformation of chromosome III in both mating types. We discovered a mating-type-specific conformational difference in the left arm. Deletion of a 1-kb subregion within the RE, which is not necessary during switching, abolished mating-type-dependent chromosome folding. The RE is therefore a composite element with one subregion essential for donor selection during switching and a separate region involved in modulating chromosome conformation.

INTRODUCTION

Budding yeast has two mating types: *a* and *α*, determined by the *MAT* locus, located on the right arm of chromosome III. The *MAT* locus expresses the mating-type-specific transcription factors *MAT_α1p* and *MAT_α2p* in *MAT_α* cells and *MAT_a1p* and *MAT_a2p* in *MAT_a* cells. These transcription factors are responsible for establishment of the *MAT_a* or *MAT_α* mating type. Besides the active *MAT* locus, chromosome III contains a silent copy of the *MAT_α* allele near the left telomere at *HML_α* and a silent copy of

MAT_a near the right telomere at *HMR_a*. The silent copies of the *MAT* locus are important for the cell to switch mating type. Mating-type switching is initiated by the HO endonuclease that generates a DNA double-strand break at the *MAT* locus. This break is then repaired by gene conversion with either *HML_α* or *HMR_a* as donor sequence (Haber, 2012).

The mating-type switching process is highly directional. *MAT_a* cells favor to switch to the *MAT_α* mating type using *HML_α* as a donor, whereas *MAT_α* cells switch to the *MAT_a* mating type using *HMR_a*. The mechanisms for mating-type-specific directionality of the gene conversion reaction at *MAT* are only partially understood and two phenomena are known to play a role. First the left arm of chromosome III is unusually refractory to recombination, both for mating-type switching and for gene conversion events in general (Haber, 2012; Wu and Haber, 1995). Second, the recombination enhancer (RE), a *cis*-acting element located on the left arm, is required to activate the left arm for switching in *MAT_a* cells (Szeto et al., 1997; Wu and Haber, 1996). The RE is composed of two highly conserved Mcm1p/*MAT_α2p* binding sites (DPS1 and DPS2; Szeto et al., 1997; Wu et al., 1997) and three arrays of binding sites for the Forkhead transcription factor FKH1p (Sun et al., 2002). The left 700-bp portion of the RE containing DPS1 and the FKH1p binding site arrays is essential and sufficient for the usage of the left arm during mating-type switching in *MAT_a* cells. The right most ~1,400 bp, which includes DPS2 but no FKH1p binding sites, has a modest effect on left-arm usage in *MAT_a* cells but is not essential, and its role is not known.

In *MAT_a* cells, the RE is in an open chromatin state and binds Forkhead transcription factors that contribute to preferential activation of the left arm for the mating-type switching reaction (Sun et al., 2002). The FHA domain of FKH1 binds phosphoserine and phosphothreonine residues that accumulate at double-strand break sites in *S. cerevisiae* (Li et al., 2012). It is thought

that FKH1 binds to the RE and forms a physical bridge to the *MAT* locus after it has been cleaved by HO. In *MAT α* cells the RE is inactivated by binding of the Mcm1p/*MAT α 2p* repressor complex that positions nucleosomes along the RE, preventing Fkh1p binding (Szeto et al., 1997; Weiss and Simpson, 1997; Wu et al., 1998a).

The mechanisms that contribute to the general inaccessibility of the left arm for recombination and the mode of action of the RE in *MAT α* cells are not understood in detail. One long-standing hypothesis is that the spatial conformation or sub-nuclear positioning of the left arm is somehow preventing it from engaging in recombination. In this model, the RE would re-position the left arm in *MAT α* cells specifically to make it available for gene conversion with the *MAT* locus (Haber, 1998a, 2012). The existence and role of pre-folding of chromosome III to the directionality of the mating-type switch has been debated, because the motion of *HML α* was mating type and RE dependent in strains disomic for chromosome III (Bressan et al., 2004), but in contrast tethering the *HM* loci to *MAT* did not alter donor preference (Simon et al., 2002). Also, nuclear positioning of the mating-type loci did not seem to differ in *a* and *α* cells (Bystricky et al., 2009), while mating-type-specific features of the folding of chromosome III could be seen in a subset of cells (Lassadi et al., 2015).

Here, we determined the three-dimensional (3D) organization of chromosome III at 4- to 8-kb resolution in non-switching strains by comprehensive mapping of long-range chromosomal interactions using Hi-C, 5C, and live-cell imaging. We discovered that chromosome III has a mating-type-dependent spatial conformation, with the left arm interacting more frequently with the centromere-proximal region up to the *MAT* locus in *MAT α* cells, whereas the left arm is more extending away from the centromere in *MAT α* cells. Interestingly, deletion of the left portion of the RE or of *FKH1* affects the conformation modestly only in *MAT α* cells, while deletion of the right portion of the RE strongly affects the conformation in both *MAT α* and *MAT α* cells leading to a conformation that is highly similar in both mating types. Our results firmly establish cell-type-specific folding of this chromosome, provide new insights into the role of the RE in chromosome structure, and show that the RE is composed of functionally distinct elements. Further, our results reveal that a single DNA element can have widespread and large-scale effects on chromosome folding, which may be a general phenomenon in larger genomes as well.

RESULTS

Genome-wide Chromatin Interaction Maps for *MAT α* and *MAT α* Cells

To investigate the conformation of the yeast genome, we performed Hi-C on exponentially growing cultures of both *MAT α* and *MAT α* cells as described previously (Belton et al., 2012; Lieberman-Aiden et al., 2009). Figure 1A shows genome-wide chromatin interaction maps for both cell types. Visual inspection of the heatmaps reveals that overall features of chromosome and nuclear organization are very similar in both mating types and consistent with previous studies. First, the interaction maps from both mating types display the characteristic Rabl configuration of chromosomes. In this conformation, all centro-

meres are clustered together at one side of the nucleus with the arms running in parallel toward the other side. In yeast, this is known to be facilitated by tethering of centromeres to the spindle pole body and the resulting Rabl arrangement has been directly observed by imaging as well as by 3C and previous genome-wide chromatin interaction analysis (Berger et al., 2008; Dekker et al., 2002; Duan et al., 2010; Jin et al., 1998, 2000; Tjong et al., 2012). In addition, as a result of tethering to the spindle pole body, the chromosomes are kinked at the centromere with the pericentromeric parts of the arms running closely and in a parallel fashion alongside each other away from the nuclear periphery. This is visible in the Hi-C maps by the cross-shaped interaction patterns around each centromere (Figures 1C and 1D). Similar cross-shaped patterns are present at each centromere-centromere interaction, indicating that the pericentric domains of all 32 arms run parallel to each other for up to 50 kb (Zimmer and Fabre, 2011). A further indication of the Rabl organization is the depletion of interactions between centromeres and more distal portions of chromosome arms. This observation is consistent with predictions based on a polymer model for yeast chromosome folding proposed by Tjong et al. (2012). In this model, volume exclusion effects by which arms of each chromosome are forced to extend into the nucleus are predicted to reduce their probability of interacting with the centromere. Additionally, we also observe that short chromosome arms are enriched for interactions with other short arms but are depleted for interactions with long chromosome arms (Figure S1A). This has also been observed before (Duan et al., 2010; Therizols et al., 2010) and is again consistent with the model proposed by Tjong et al. (2012), where volume exclusion effects near the centromeres are predicted to push the long chromosomes further out into the nuclear volume. Second, telomeres interact with one another more frequently than would be expected for the genomic distance between them (Agmon et al., 2013; Duan et al., 2010). This is consistent with observations that telomeres cluster and are frequently found near the nuclear periphery (Berger et al., 2008; Bystricky et al., 2009; Gotta et al., 1996; Trelles-Sticken et al., 2000).

The Folding of Chromosome III Is Mating Type Dependent

To compare the spatial organization of the genome in *MAT α* and *MAT α* cells, we calculated the log₂ ratio of the two Hi-C interaction maps and plotted the results again as a heatmap (Figure 1A, right). A weak global pattern of differences in inter-chromosomal centromere-arm interactions is observed that can be explained by small differences in noise levels of very-low-level inter-chromosomal interactions between experiments and is also observed in comparisons between biological replicates (Figure S1B). This is not observed for intra-chromosomal interactions that are less susceptible to fluctuations of noise since the interaction values are orders of magnitude higher than inter-chromosomal contacts.

Comparison of interaction maps for each chromosome reveals that there are very few intra-chromosomal differences in conformation, with log₂ ratios centered on zero (Figure 1B). Interestingly, chromosome III has the most differences in chromatin interactions between the mating types, and these differences

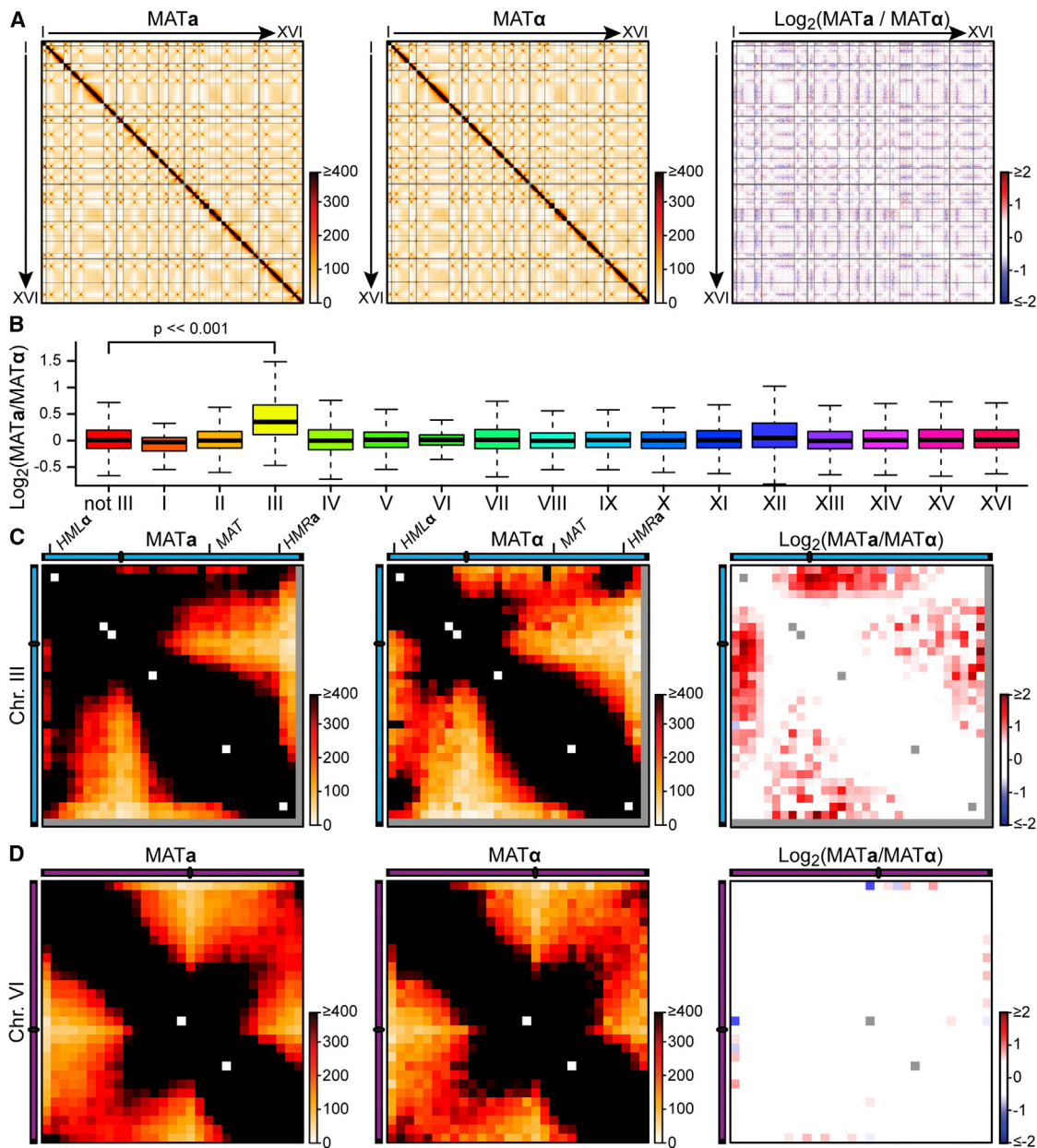


Figure 1. Global Chromosome Conformation in Both *MATa* and *MATα* Cells

(A) The left and middle panel show Hi-C data obtained with *MATa* and *MATα* cells, respectively. Data from two biological replicates were pooled and corrected using the iterative coverage correction method at 10-kb resolution, and the total number of counts has been normalized for each data set. The chromosomes are sorted on both axes by the chromosome number. The right panel displays the $\text{Log}_2(\text{MATa} / \text{MAT}\alpha)$ ratio.

(B–D) Zoom in to chromosomes III and VI. Left and middle panel: Hi-C data for *MATa* and *MATα* cells. Right panel: heatmaps displaying the $\text{Log}_2(\text{MATa} / \text{MAT}\alpha)$ ratios to highlight the difference in chromatin interactions in the two mating types.

are statistically significant compared to those of the other chromosomes combined. Therefore, we analyzed the conformation of chromosome III in more detail (Figure 1C). In both mating types, we observe general conformational features that are shared with other chromosomes: a general inverse relationship between interaction frequency and genomic distance and a cross-shaped pattern of interactions around the kinked centromere. In addition, in both mating types, we observe prominent

interactions between the heterochromatic silent *MAT* loci (*HML* and *HMR*) located on opposite ends of the chromosome (Figure 1C), which have been detected and characterized in detail previously (Bystricky et al., 2005, 2009; Dekker et al., 2002; Miele et al., 2009).

The major difference in the conformation of chromosome III between the two mating types is that the distal portion of the left arm, containing *HML* and the RE, is interacting more frequently

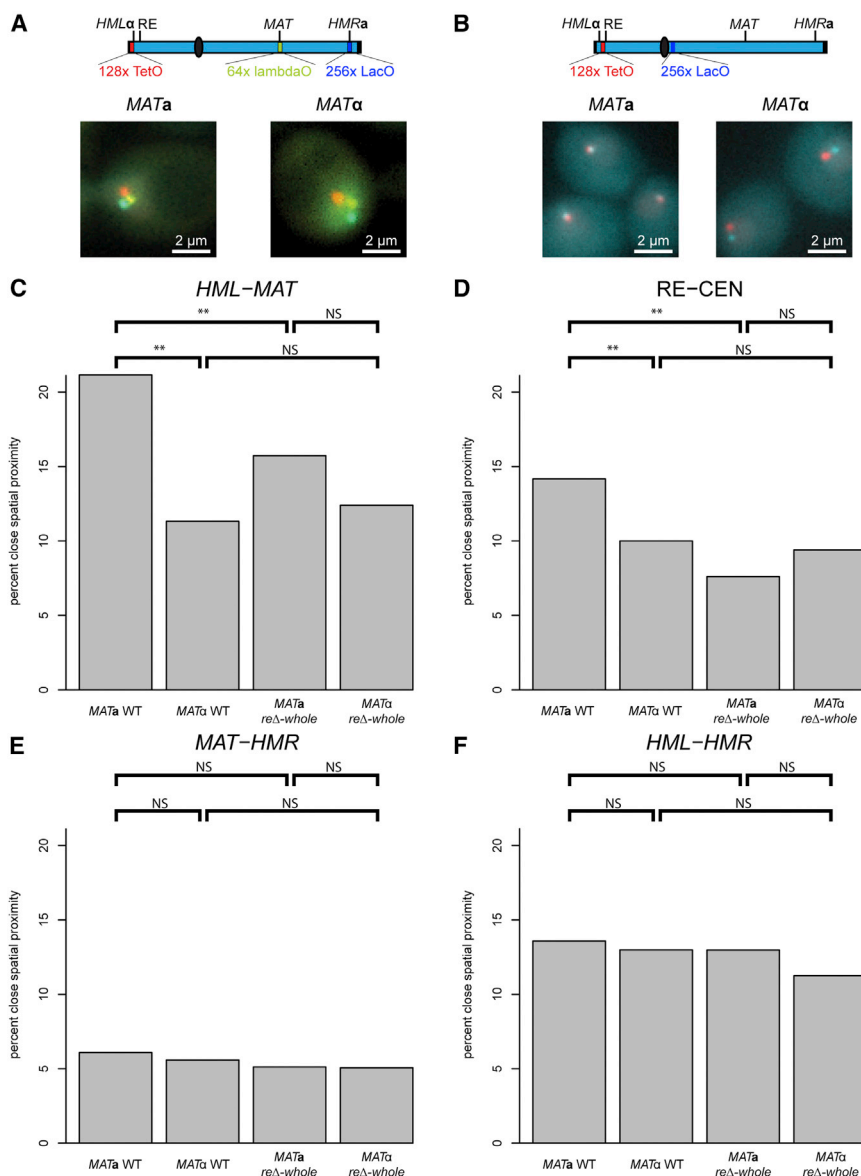


Figure 2. Live-Cell Microscopy Validates Mating-Type-Dependent Conformation of Chromosome III

(A and B) Schematic of chromosome III indicating the locations of the operator arrays that were used to measure the distances between *HML*, *MAT*, and *HMR* (A) and RE and the centromere (Cen) (B). Representative images are shown below the schematic. Scale bar, 2 μ m.

(C–F) Percentage of co-localization, defined as the percentage of distances between pairs of loci that are less than or equal to 250 nm. Statistical significance was determined by bootstrapping analysis (see [Supplemental Experimental Procedures](#)). NS, not significant. ** $p \leq 0.002$ after Bonferroni correction for multiple testing. Co-localization was determined for *HML* and *MAT* (C), RE and Cen (D), *MAT* and *HMR* (E), and *HML* and *HMR* (F), in *MATa* and *MAT α* cells and in *MATa* and *MAT α* cells with the entire RE deleted.

two sets (*MAT α* and *MATa*) of strains to allow us to measure the distance between specific loci on chromosome III in live cells using microscopy. For one set, we inserted an array of 128 TetO operators just to the left of the RE (chrIII: 26,969–27,433) and an array of 256 LacO operators just to the right of the centromere (chrIII: 115,899–116,396). In this set, we also expressed TetR-mRFP and LacI-CFP fusion proteins that bind to the corresponding operator arrays and fluoresce in live cells to indicate their position (Figure 2B). For the other set, we inserted 128 TetO operators at *HML* (chrIII:15,160–15,773), 64 LambdaO operators at *MAT* (chrIII:197,197–197,310), and 256 LacO operators at *HMR* (chrIII:294,898–295,245). We expressed TetR-mRFP, LambdaR-YFP, and LacI-CFP to visualize *HML*, *MAT*, and *HMR*, respectively. We then measured three-

dimensional distances between these loci in both *MAT α* and *MATa* cells (Figures 2C–2F) and determined the percentage of each pair of loci that are in relative close spatial proximity (distance <250 nm, see [Supplemental Experimental Procedures](#)). We found that both the RE is co-localized more with the centromeric region, and *HML* is co-localized more with *MAT* in *MATa* as compared to *MAT α* cells. Similar mating-type-dependent differences in the distance between RE and CEN were observed when analysis was restricted to G1 cells, indicating that the difference between *MAT α* and *MATa* cells was not due to differences in cell-cycle time or progression (Figure S1). No significant mating-type-dependent differences were observed in frequency of close spatial juxtaposition of *MAT* with *HMR* and of *HML* with *HMR*.

with an area that extends from the centromere to the *MAT* locus on the right arm (Figure 1C). This is visible directly in the Hi-C interaction maps and more pronounced in the Log2 difference heatmap. There is also an increase in interactions between the end of the right arm and this same region from the centromere to *MAT* (Figure 1B). This is probably at least in part driven by the *HML*-*HMR* interaction. Analysis of the similarly small chromosome VI revealed no mating-type-specific differences (Figure 1D).

A more frequent association of the left arm with the centromere proximal region of the chromosome in *MATa* cells should also affect the interactions between this arm and arms of other chromosomes. Indeed, we find that the left arm in *MATa* cells interacts less with other chromosome arms than it does in *MAT α* cells (Figure S1A).

To verify the mating-type-dependent difference in chromosome conformation using an independent method, we made

From these analyses, we conclude that chromosome III is the only chromosome that is folded in a mating-type-dependent

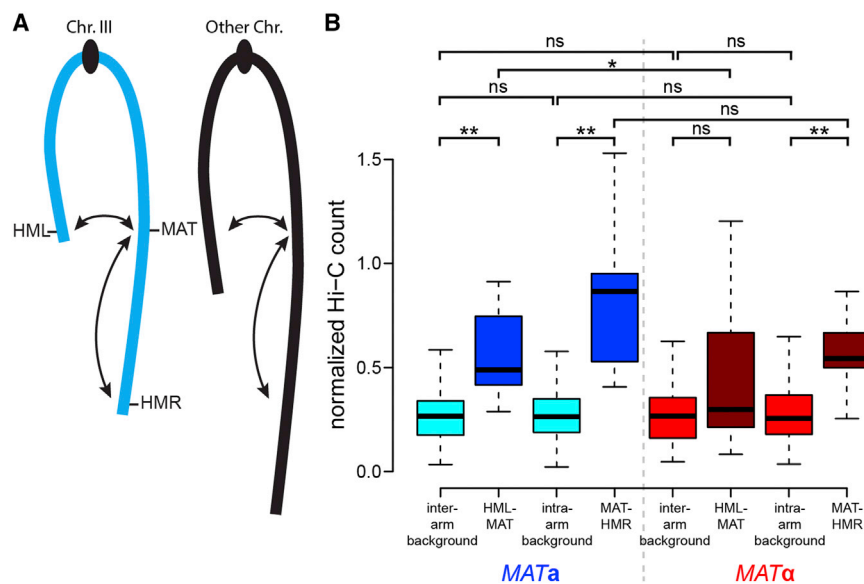


Figure 3. Interaction Frequencies between HML and MAT and HMR and MAT in MATa and MATα Cells

(A) Schematic of how expected interaction frequency for HML-MAT and HMR-MAT was calculated. Left shows a schematic of chromosome III, and the black arrows indicate the contact frequencies measured between HML and MAT and between HMR and MAT. The right is a schematic of other short and medium arm chromosomes. The black arrows that are between the two arms are interactions collected from these chromosomes that are at the same position from the centromere as HML and MAT. Black arrows along a single arm indicate interaction frequencies that are separated by the same genomic distance as HMR is from MAT. These interactions were collected from other short chromosome arms (chr1R, chr9R, chr8L, chr6R, chr12L, chr1L, chr5L, chr6L, chr14R) and used as background estimates (“inter-arm background” and “intra-arm background”).

(B) Boxplots of sets of interactions indicated in (A) and collected on chromosome III in MATa and

MATα cells and from other short chromosomes (“inter-arm background” and “intra-arm background”). The y axis is the interaction frequency between the indicated loci. HML and MAT, as well as HMR and MAT interact more frequently than comparably positioned loci on other chromosomes. HML interacts more frequently with MAT in MATa as compared to MATα. The difference in contact probability was tested using the rank-sum test and Bonferroni corrected for multiple comparisons. A single asterisk indicates a p value <0.05, and a double asterisk indicates a p value <0.001 after Bonferroni correction for multiple testing.

manner, through differential co-localization of the left arm with a domain from the centromere to the MAT locus.

Interactions between MAT and HML Are More Frequent in MATa Cells

It has been hypothesized that a mating-type-specific conformation would exist such that in MATa cells the MAT locus would be closer to HML, or alternatively, so that in MATα cells the left arm would be somehow sequestered away (Haber, 2012). Given that HML is further away from MAT than HMR in the linear genomic sequence of chromosome III, one naively would expect that HMR would have a higher probability of interacting with MAT than HML. However, the Rab1 orientation of the chromosomes adds an additional level of structure that must be considered. Our Hi-C data allowed us to test and quantify this directly. We tested whether pairs of loci that are on separate arms of the same chromosome (excluding chromosome III) and are located the same distance from the centromere as HML and MAT interact more or less frequently than pairs of loci that are on the same chromosome arm and positioned the same distance from each other as MAT and HMR (Figure 3A). Interestingly, we observe that there is no difference in the frequency of interaction for these two types of interactions along chromosomes other than III (compare Figure 3B “inter-arm background” to “intra-arm background”).

The analysis above predicts that in the absence of any chromosome III-specific constraints HML and HMR would both have the same probability of interacting with MAT. In Figure 3B, we plot the distribution of normalized Hi-C counts for a region that is up to 10 kb away from HML with a 20-kb region around the MAT locus. In MATα cells, we find that the contact probabilities between HML and the MAT locus are very similar to those between other pairs of

loci located on other arms and 100 kb from their respective centromere. Thus, in MATα cells the interaction between HML and MAT is as expected from a Rab1 orientation. Interestingly, and consistent with the results described above, in MATa cells HML interacts significantly more frequently with MAT than expected for a Rab1 orientation, as indicated by the comparison to the interaction frequency of other pairs of loci located on other arms at equidistant positions from the centromere. Further, HML interacts significantly more frequently with MAT in MATa cells as compared to MATα cells. Thus, the mating-type-dependent conformation of chromosome III leads to more frequent contacts between HML and MAT in MATa cells specifically.

To determine whether HMR and MAT, which are located on the same arm, interact more frequently than expected based on their genomic site separation, we compared their interaction frequency with that of other pairs of loci on other chromosome arms that are separated by a similar genomic distance. In both mating types, we find that HMR and MAT interact more frequently than expected. Possibly this is driven at least in part by the interaction between HMR and HML.

We conclude that the mating-type-dependent conformation of chromosome III leads to an increased probability in MATa cells that MAT interacts with HML, the preferred donor during mating-type switching in that cell type. We note, however, that even in MATa cells MAT interacts more frequently with HMR, indicating that the spatial proximity prior to switching may contribute to but is not sufficient for the strong donor selection preference observed during mating-type switching.

5C Analysis of Chromosome Organization

To further investigate the conformation of chromosome III, we performed 5C. We designed 5C probes to HindIII restriction

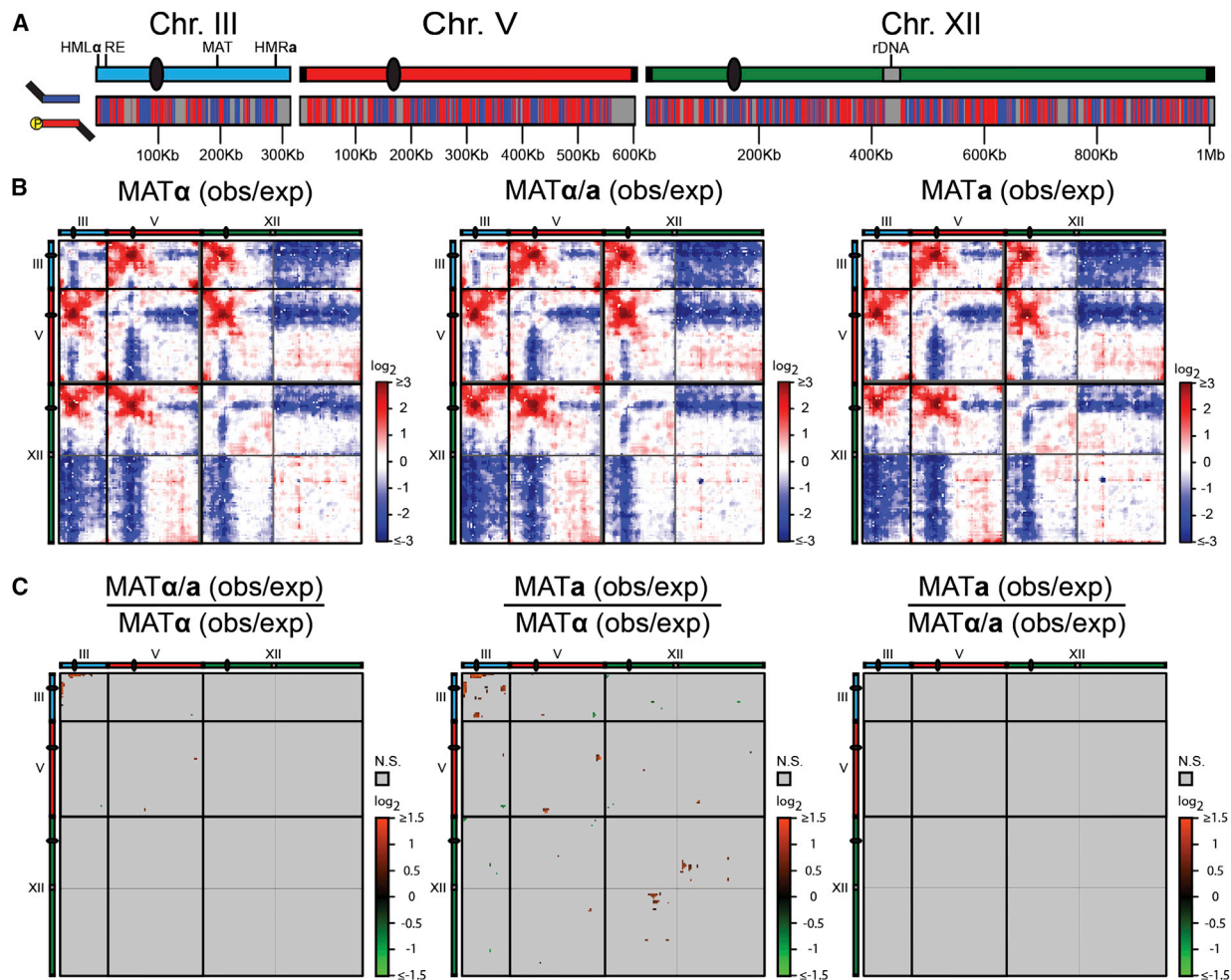


Figure 4. Mating-Type-Specific Chromosome Conformation Detected by 5C

(A) 5C probe positions are indicated below the depictions of chromosomes III, V, and XII. Blue, forward primers; red, reverse primers.

(B) 5C data normalized by the genomic distance-dependent expectation and then binned as in Figure 1. *MATα* cells (left), *MATa/a* cells (middle), and *MATa* cells (right).

(C) \log_2 ratio of normalized 5C signal obtained with the indicated pairs of strains. Light gray indicates bins that did not display a significant difference in interaction frequency (5% FDR). Dark gray represents regions for which no 5C data were obtained. Bins with color are those that showed a significant difference between the two samples at a 5% FDR. The color value of significant bins is the \log_2 ratio of the median distance-normalized 5C signal for that bin in strain one and that of strain two. Left: comparison between *MATa/a* and *MATα* cells. Middle: comparison between *MATa* and *MATα* cells. Right: comparison between *MATa* and *MATa/a* cells.

fragments on chromosome III as well as for two control chromosomes V and XII (Figure 4A; Tables S1, S3, and S4). 5C provides high-resolution interaction maps in a more cost-effective manner than genome-wide Hi-C because it focuses analysis on only a selected section of the genome (Dekker et al., 2013; Dostie et al., 2006). Forward and reverse 5C probes were designed on restriction fragments in an alternating fashion (Lajoie et al., 2009). The combination of these 5C probes can detect 80,784 chromatin interactions occurring within and between the three selected chromosomes (Figure 4B).

5C interaction maps were obtained for three replicates of exponentially growing *MATa*, *MATα*, and diploid cells. To remove any small biases due to minor variations in 5C primer efficiency, chromatin digestion and ligation efficiency, or DNA

sequencing, from the 5C data, we used the iterative coverage correction method ICE (Imakaev et al., 2012) to balance the 5C interaction matrices. Previously, we successfully applied ICE to 5C maps of individual chromosomes as well (Naumova et al., 2013). Analysis of the Hi-C interaction maps for chromosomes III, V, and XII indicates that the assumption of ICE of equal visibility is reasonably met for this subset of the genome. Table S2 and Figure S4 summarize all data sets generated for this study.

The most prominent feature in chromatin interaction data sets is the high interaction frequency of pairs of loci that are very close to each other in the linear genome (Dekker et al., 2013). This signal decays with increasing genomic distance. This results in a strong signal along the diagonal in the interaction heatmap that can

obscure additional features (Figure 1A; Figures S2 and S3B). To reveal additional interaction patterns, we removed the distance-dependent 5C signal. This was done by first calculating the data-set-wide average relationship between genomic distance and interaction frequency (Experimental Procedures; Supplemental Experimental Procedures) to estimate the expected interaction frequency of any pair of loci given their genomic separation (Figure S3B; Supplemental Experimental Procedures). We then calculated the log ratio of the observed data and the expected values for each pair of genomic loci (Figure 4B).

Visual inspection of the distance-corrected interaction maps for these cell types again suggests that global chromosome conformation in these strains is very similar (Figure S4). We also confirm the depletion of interactions between the centromeres and chromosome arms, and the prominent *HML-HMR* interactions on chromosome III. The resulting 5C interaction maps highly correlate with those obtained with Hi-C experiments (Figure S5A).

Quantification of Mating-Type-Specific Differences in Conformation of Chromosome III

To more rigorously analyze cell-type-dependent chromatin interaction frequencies, we developed a method to identify statistically significant differences between two strains (Experimental Procedures; Supplemental Experimental Procedures; Figure S6A). Briefly, we first binned the 5C data ($\text{Log}_2[\text{observed/expected}]$ values) into overlapping 30- by 30-kb bins (overlap 10 kb), with a median coverage of ~ 27 pairwise chromatin interactions pooled from all three biological replicates. Next, we tested whether distance-corrected 5C signals in each of the bins are significantly different between two strains at a 5% false discovery rate (FDR) threshold (Figure S6A). We then plotted only the significant differences in chromatin interactions between two strains in a heatmap where each pixel indicates the fold difference in the median 5C signal of each 30-kb bin in strain 1 as compared to strain 2 (Figure 4B). Very few significant differences in intra-chromosomal interactions were observed between biological replicates of the same strain indicating a low false-positive rate (Figure S6B).

We performed three pairwise comparisons: diploid versus *MAT α* cells, *MATa* versus *MAT α* cells, and *MATa* versus diploid cells. Overall, we identified a limited set of statistically significant differences between the three cell types. Two sets of cell-type-specific chromatin interactions stand out. First, the regions flanking the rDNA locus interact significantly more frequently in *MATa* cells as compared to *MAT α* cells. This is likely due to the presence of a lower number of rDNA repeats in these *MATa* cells. This is not unexpected since rDNA size in *S. cerevisiae* is known to vary between populations (Rustchenko et al., 1993). Interaction frequencies between the rDNA flanking regions are not significantly different when comparing *MATa* to diploid cells or when comparing *MAT α* to diploid cells. Given that this diploid strain was produced by mating both the haploid strains studied here, the interactions between the chromatin segments flanking the rDNA locus are at an intermediate level compared to *MATa* and *MAT α* cells because the 5C interaction signal from each of the homologous chromosomes averages out. This intermediate signal is subsequently not different

enough to be called significant from either haploid strain using our 5% FDR threshold.

Second, the conformation of chromosome III is significantly different in *MAT α* cells compared to *MATa* or diploid cells, with the latter being overall similar to *MATa* cells. In both *MATa* and diploid cells, a portion of the left arm, including *HML* (chrIII: 0–50,000), interacts frequently with the central portion of the chromosome (chrIII: 50,000–230,000), containing the centromere and the centromere proximal part of the right arm as well as the *MAT* locus. In *MAT α* cells, these interactions are significantly lower (Figures 4B and 4C). This difference was also observed in two independent strains with a different genetic background (w303; Figure S5B). Furthermore, and consistent with the Hi-C data sets, we again observe that in *MATa* cells a 50-kb region at the telomeric end of the right arm (chrIII: 240,000–290,000) interacts with a region just around the centromere up to the *MAT* locus (chrIII: 70,000–185,000) (Figure 5).

The Recombination Enhancer Is Responsible for the Mating-Type-Dependent Conformation of Chromosome III

It has been proposed that the RE influences the conformation of chromosome III in a mating-type-dependent manner so that in *MATa* cells the left arm becomes available for recombination during mating-type switching (Haber, 1998b). To test whether the RE indeed modulates the spatial organization of chromosome III, we deleted the entire RE positioned between *KAR4* and *SPB1* (chrIII: 28,988–31,140) (Figure 7E) in *MATa* and *MAT α* cells. This deletion (*re Δ -whole*) removes *DPS1* and *DPS2*, as well as all three Fkh1p binding site arrays. We then performed 5C on non-switching exponentially growing cultures to assess the conformation of chromosome III. Interestingly, deletion of these elements ablated the mating-type-specific conformation observed in wild-type cells (Figure 5B). We also showed the loss of mating-type-specific differences in interactions by live-cell microscopy: we found no significant mating-type-dependent difference in the frequency of close spatial proximity of the left arm and the centromere and of *HML* and *MAT* in *MATa* and *MAT α* cells carrying the RE deletion (Figures 2C–2F, compare RE deletion to WT). Therefore, the RE plays a major role in modulating the mating-type-dependent conformation of chromosome III. Interestingly, the conformation of the chromosome in the RE deletion strains is different from the wild-type in both mating types (see below). The conformation of chromosomes V and XII was not affected by the deletion (Figures S2 and S4).

The Right Portion of the RE Is the Major Driver of Mating-Type-Dependent Chromosome Conformation

The 700-bp fragment toward the left end of the RE containing the Fkh1p binding sites and the *DPS1* operator has been functionally defined as the minimal RE that is required and sufficient for selecting *HML* during mating-type switching in *MATa* cells (Haber, 1998a; Sun et al., 2002; Wu and Haber, 1996). Therefore, we hypothesized that this left portion of the RE could be the driver of the mating-type-dependent differences in the conformation of chromosome III. To test this, we deleted only the left portion of the RE (chrIII: 28,988–29,852) in *MATa* and *MAT α* cells and

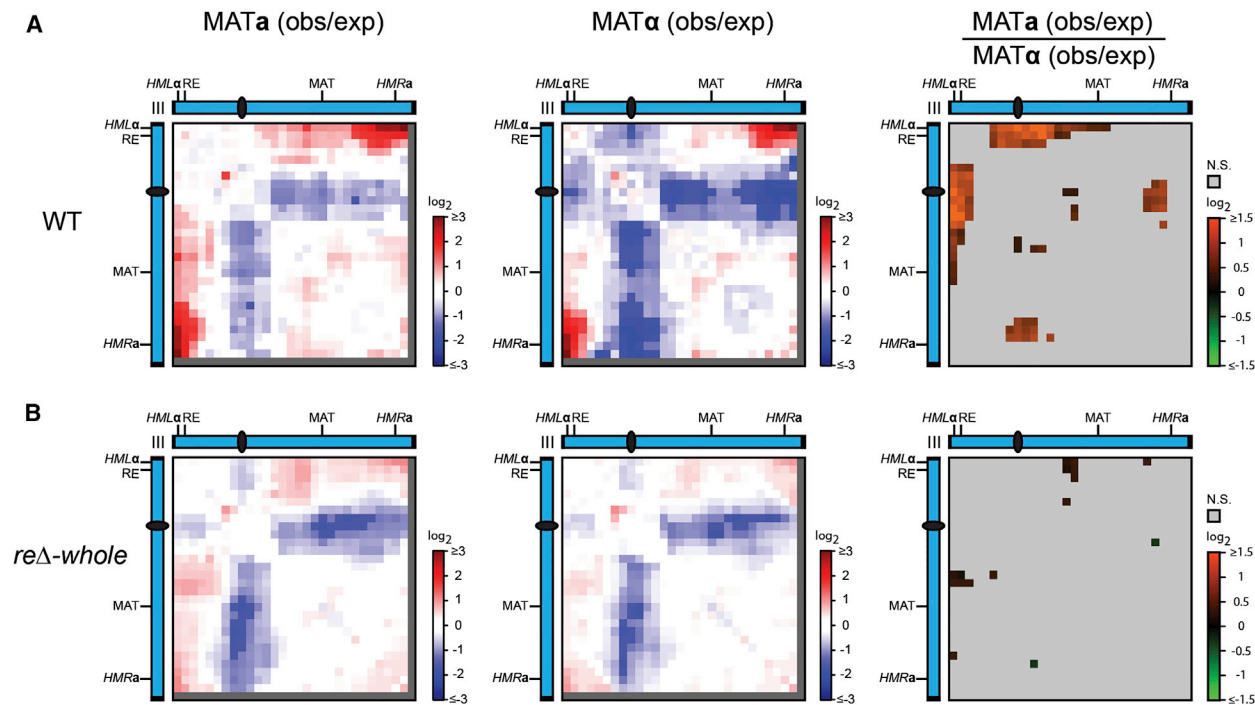


Figure 5. The Recombination Enhancer Is Responsible for Mating-Type-Specific Chromosome Conformation

(A) Left: 5C interaction frequencies obtained with *MATa* cells, normalized for distance-dependent interaction frequency. Middle: 5C interaction frequencies obtained with *MAT α* cells, normalized for distance-dependent interaction frequency. Right: heatmap displaying the log₂ ratio of significantly different 5C interaction frequencies in *MATa* and *MAT α* cells (5% FDR; as in Figure 4).

(B) As in (A), for *MATa* and *MAT α* cells in which the entire RE was deleted.

performed 5C in exponentially growing cultures (Figure 6A). Surprisingly, deletion of this region did not abolish the mating-type-specific conformation of chromosome III confirming previous observations in living cells (Lassadi et al., 2015). We did observe some changes in the conformation of the chromosome in *MAT α* cells. In *MAT α* cells, the chromosome adopts a more “*MATa*-like” conformation with the left arm interacting more frequently with the centromere proximal region. *MAT* and the end of the right arm also interact more frequently with this region (Figure 7B). However, this change is small and the main significant differences in chromosome conformation observed between *MATa* and *MAT α* cells are maintained.

To further study any role of the left portion of the RE, we deleted the *FKH1* gene. 5C analysis showed that the absence of Fkh1p has a very similar phenotype as the RE-left deletion, and the mating-type-specific conformation of the left arm is maintained (Figure 6B). We note that in the *FKH1* deletion the conformation of chromosome III is modestly affected in *MAT α* cells only, similar to the effect of deletion of the left part of the RE. This is surprising as Fkh1p is not thought to bind the RE in *MAT α* cells. One explanation could be that nucleosome-mediated exclusion of Fkh1p from the left part of RE *MAT α* cells is not complete, and that any effect of this element on the conformation of chromosome III in *MAT α* cells is mediated through this binding of Fkh1p.

Given that the left portion of the RE did not contribute to most of the structural differences of chromosome III between

the mating types, we reasoned that the right-most portion of the RE (chrIII: 29,852–31,140) might therefore be involved. We deleted this region in *MATa* and *MAT α* cells and performed 5C on exponentially growing cultures. In this mutant, the conformation of chromosome III is the same in both mating types and very similar to the conformation observed in strains that have the entire RE deleted (Figures 5B, 7A, and 7C). We conclude that the right portion of the RE is the major element that drives the mating-type-specific conformation of the chromosome III.

The RE Modulates the Conformation of Chromosome III in Both Mating Types

We noted that the mating-type-independent conformation of chromosome III in the RE deletion strains was different from the conformation observed in either wild-type *MATa* or *MAT α* cells. To examine this in more detail, we quantified the difference in conformation in WT and mutant cells of the same mating type (Figures 7B–7D). In *MATa* cells, the *re Δ -whole* mutant resulted in a statistically significant reduction in interactions between the distal part of the left arm with the centromere-*MAT* proximal domain. Conversely, deletion of the entire RE in *MAT α* cells resulted in a statistically significant increase in interactions between the left arm and the centromere-*MAT* proximal region as compared to WT *MAT α* cells. Given the *HML* and *HMR* interactions, the right arm also interacts more strongly with this region (see above). In addition, a region between the centromere and

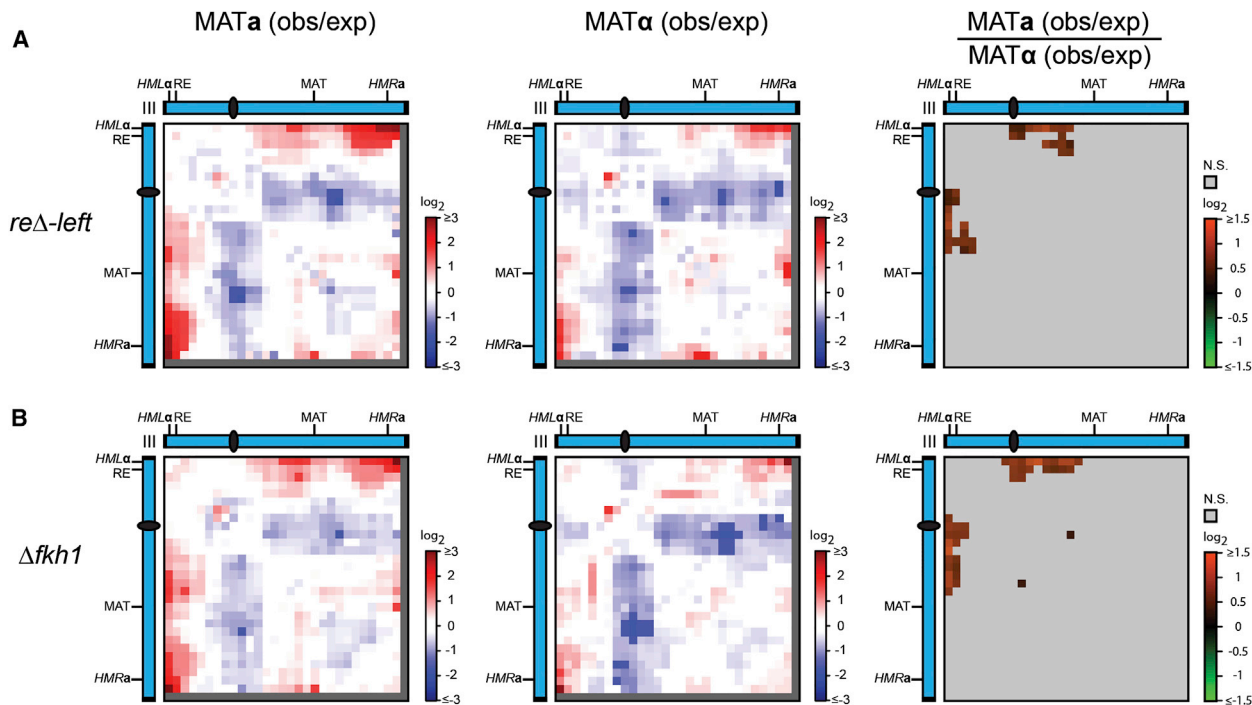


Figure 6. The Left Part of the Recombination Enhancer Only Plays a Minor Role in the Conformation of Chromosome III

(A) Left: 5C interaction frequencies obtained with *MATa* cells in which the left portion of the RE was deleted, normalized for distance-dependent interaction frequency. Middle: 5C interaction frequencies obtained with *MATα* cells in which the left portion of the RE was deleted, normalized for distance-dependent interaction frequency. Right: heatmap displaying the log₂ ratio of significantly different 5C interaction frequencies in *MATa* and *MATα* cells in which the left portion of the RE was deleted (5% FDR; as in Figure 4).

(B) As in (A), for strains in which *FKH1* was deleted.

the *MAT* locus interacts more strongly with the centromere when the RE is deleted (Figure 7D). In *MATa* cells, the *reΔ-right* mutation also causes the conformation to lose some of its *MATa* characteristics (Figure 7C), but it again does not convert to a complete “*MATα*-like” conformation (Figure S7). The same is true for *MATα* cells, where a loss of *MATα* characteristics was observed (Figure 7C), but the conformation did not converge to an “*MATa*-like” state (Figure S7). Therefore, in the *reΔ-right* and *reΔ-whole* deletion strains, the chromosome adopts a third and distinct conformation from either the wild-type *MATa* or *MATα* conformations.

Consistent with the analysis shown in Figure 6, deletion of the left portion of the RE had only an effect on the conformation of chromosome III in *MATα* cells. In the mutant, we observed an increased interaction between the centromere and both the left and right arms. Unexpectedly, we observed a reduction in the *HML-HMR* interactions in both *MATa* and *MATα* cells when either the entire RE or the right portion of the RE is deleted (Figures 7C and 7D). Whether this is a direct or indirect effect is currently unknown.

These analyses reveal that the right portion of the RE, encompassing a single *Mcm1p/MATα2p* site, plays a major and critical role in modulating the conformation of chromosome III in a mating-type-dependent manner. This element imposes different structural constraints on the chromosome in *MATa* and *MATα* cells so that in the absence of this element the chromosome

adopts a different, less constrained, mating-type-independent conformation.

DISCUSSION

It has long been hypothesized that the conformation of chromosome III would be mating type specific (Haber, 2012). Our Hi-C and 5C studies now firmly establish that the three-dimensional organization of chromosome III, but not of other chromosomes, is dependent on the mating type of the cell. The left arm is either juxtaposed near the central part of the chromosome from the centromere up to the *MAT* locus in *MATa* cells or is in a more extended configuration projecting away from the centromere in *MATα* cells. We confirmed this differential positioning by live-cell imaging. In addition, imaging studies from Bressan et al. have previously also suggested that *HML* is on average closer to *MAT* in *MATa* cells than it is in *MATα* cells (Bressan et al., 2004). Their data also indicate that *HMR* may be closer to *MAT* in *MATα* cells, a fact that our 5C data do not confirm.

As a result of the differential folding of the chromosome, in *MATa* cells *HML* is positioned more frequently near the *MAT* locus. These cells have not initiated switching, and this therefore represents a ground state of the chromosome prior to break formation at *MAT*. In *MATa* cells *HML* is the preferred donor during mating-type switching. It is tempting to propose that this conformation is involved in selecting *HML* during switching. It had been

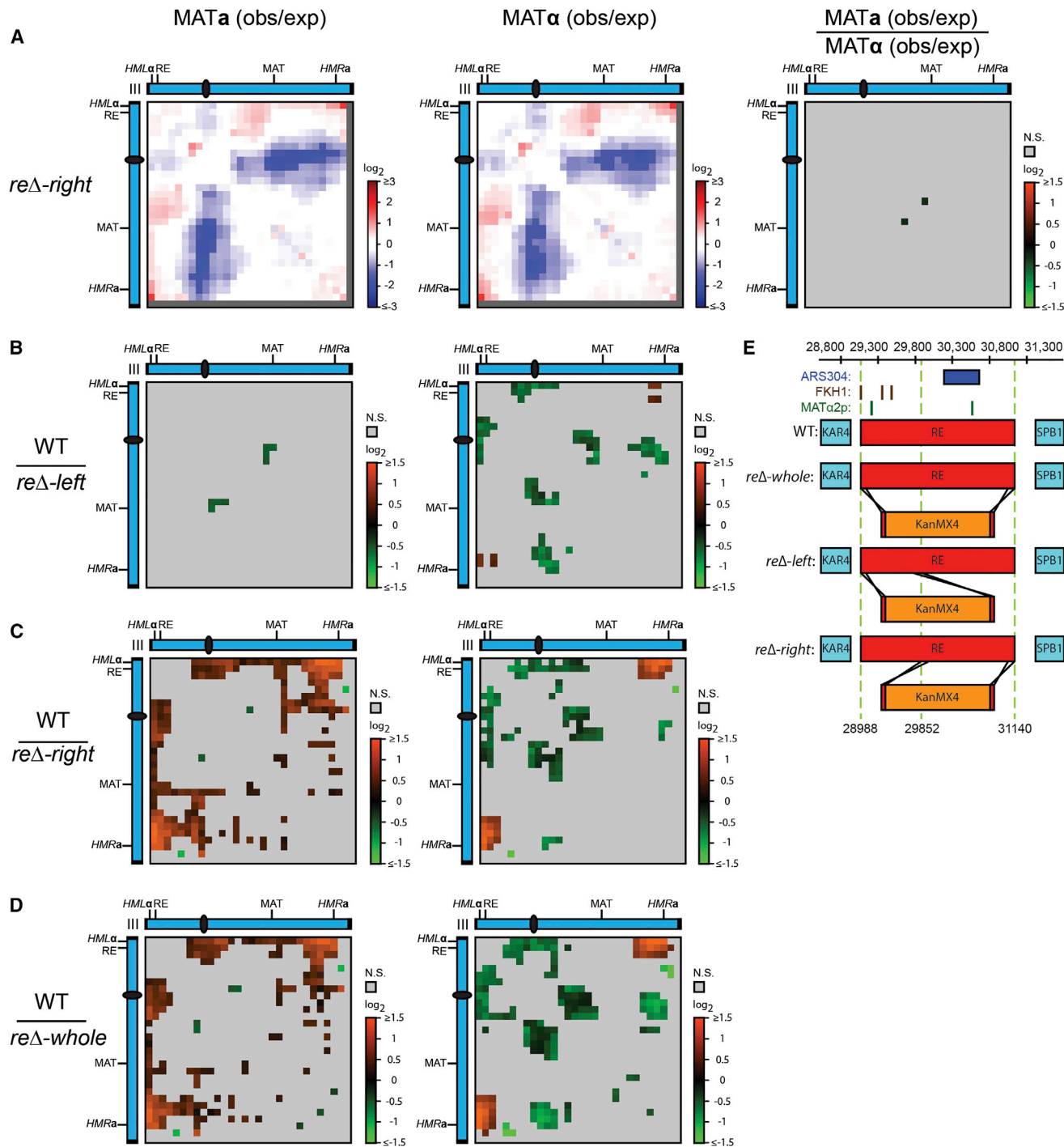


Figure 7. The Right Part of the Recombination Enhancer Is Responsible for the Conformation of Chromosome III in Both Mating Types
 (A) Left: 5C interaction frequencies obtained with *MATa* cells in which the right portion of the RE was deleted, normalized for distance-dependent interaction frequency. Middle: 5C interaction frequencies obtained with *MATα* cells in which the right portion of the RE was deleted, normalized for distance-dependent interaction frequency. Right: heatmap displaying the \log_2 ratio of significantly different 5C interaction frequencies in *MATa* and *MATα* cells in which the right portion of the RE was deleted (5% FDR; as in Figure 4).
 (B–D) Heatmaps displaying \log_2 ratio of the significantly different interaction frequencies obtained in wild-type cells and mutant cells with the same mating type (5% FDR). Left: comparisons in *MATa* cells. Right: comparisons in *MATα* cells.
 (E) Schematic of the RE's genomic context and the deletion mutants utilized in this study.

proposed that any mating-type-specific folding of the left arm of chromosome III would be dependent on the activity or the RE. Indeed, we find that a deletion of 2.15 kb that contains the RE abolishes the mating-type-specific conformation of chromosome III. Interestingly, the conformation of the chromosome differs from that in wild-type cells of either mating type, indicating that the full RE plays architectural roles in organizing the chromosome in both *MAT α* cells and *MAT α* cells. Importantly, combined with previous functional studies of the element (Haber, 1998a, 1998b), our results reveal that the RE is a composite element with the minimal, left portion of the RE acting during mating-type switching in *MAT α* cells, whereas the right portion acts as a novel chromosome architectural element in both mating types under non-switching conditions.

The Left Part of the RE Plays an Architectural Role in *MAT α* Cells Only

Previous deletion studies had identified a minimal region of 700 bp within the RE that is essential and sufficient for selecting *HML* during mating-type switching in *MAT α* cells (Wu and Haber, 1996). This region contains a single *Mcm1p/MAT α 2p* and several *Fkp1* binding sites. In *MAT α* , *Mcm1* binds to the minimal RE and, together with *Swi4/Swi6*, opens the chromatin so that *Fkh1p* can bind (Szeto and Broach, 1997; Szeto et al., 1997; Wu et al., 1998a). *Fkh1p* has been proposed to mediate direct contacts with phosphorylated histones at *MAT* upon HO-mediated DNA cleavage, and thereby bringing *HML* in close proximity to *MAT* (Li et al., 2012).

We find that the 700-bp minimal RE is not responsible for the main differences in chromosome conformation in the two mating types under non-switching conditions. Deletion of the left portion of the RE did affect some aspects of chromosome conformation in *MAT α* cells but did not abolish the overall differential folding of chromosome III.

Both 5C analysis and live imaging studies of the RE mutants showed that the left portion of the RE affected the conformation of chromosome III in *MAT α* cells instead of *MAT α* cells, which would have been predicted from switching experiments (Lassadi et al., 2015). *DPS1* and *DPS2* have been shown to repress the RE in *MAT α* cells through binding of *Mcm1p/MAT α 2p/Tup1p*. The left-most site, *DPS1*, is a stronger repressor than *DPS2* (Szeto et al., 1997). Thus, it is possible that the repressing complex recruited to *DPS1* in *MAT α* cells influences the conformation of the left arm. In this scenario, the minimal left portion of the RE acts in both mating types but in different ways: it helps recruit the left arm to *MAT* during mating-type switching in *MAT α* cells, and it modulates the conformation of the left arm in *MAT α* cells under non-switching conditions.

The Right Portion of the RE Modulates Chromosome Conformation in Both Mating Types

It was interesting that deletion of the right part of the RE changed the conformation of chromosome III in both mating types and to the same extent as deleting the entire element. The right portion of the RE contains *DPS2* as well as *ARS304*. The molecular mechanism that acts through this portion of the RE is unknown. Given that this element acts in a mating-type-dependent manner, we consider a role for *DPS2*, which binds different com-

plexes in *MAT α* and *MAT α* cells, most likely. Possibly, the binding of the *Mcm1* activator in *MAT α* cells has a different effect on chromosome conformation than the binding of the *Mcm1/MAT α* repressor in *MAT α* cells. Given that deletion of only the right portion of the RE is sufficient to abolish mating-type-dependent folding of the chromosome, comparable to deleting the full RE, the left portion of the RE by itself, in the absence of *DPS2*, does not affect chromosome conformation even though it also contains a *Mcm1/MAT α* binding site (*DPS1*). However, the left portion of the RE does affect the conformation of the chromosome in *MAT α* cells when the right portion of the RE is present. This implies functional interactions between the two portions of the RE. Possibly factors binding the minimal RE such as the *Mcm1/MAT α* complex facilitate binding of these factors to the nearby *DPS2* site in the right portion of the RE that has a lower affinity for the complex (Szeto et al., 1997). In this scenario, deleting the minimal RE reduces *DPS2* occupancy, which, in turn, could modestly affect chromosome conformation in *MAT α* cells.

The mechanisms by which the RE modulates the conformation of chromosome III are still unknown but could potentially involve tethering of the left arm to a nuclear structure such as the nuclear envelope or the nucleolus. Association of *HML* with the periphery is not different between the two mating types so it is unlikely that association with the periphery could cause this effect (Bystricky et al., 2009). Also, we do not observe a significant enrichment of interactions of the left arm of the chromosome with regions adjacent to the rDNA on chromosome XII in the Hi-C and 5C data, so it is unlikely there is an association between the left arm and the nucleolus. Better characterization of the protein complexes associated with the various parts of the RE in the two mating types will be important to start to answer this question.

Chromosome Conformation and Donor Selection during Mating-Type Switching

Previous studies on translocation events have led to the model that the spatial arrangement of chromosomes and the relative spatial proximity between loci can predispose certain translocation events upon break formation (Hakim et al., 2012; Meaburn et al., 2007; Roix et al., 2003; Zhang et al., 2012). Similarly, it has been proposed that the conformation of chromosome III could guide donor choice in the two yeast mating types (Bressan et al., 2004). Consistently, we find that the conformation of chromosome III, and especially the left arm, is distinct in the two mating types, even in non-switching conditions. In addition, in *MAT α* cells *MAT* interacts more frequently with *HML* as compared to *MAT α* cells. Thus, this would lead to the prediction that the conformation of the chromosome in *MAT α* cells would indeed favor selecting *HML* as the donor. Consistent with some role of the conformation of chromosome III in donor selection deletion of *DPS2*, located in the right portion of the RE, abolishes the mating-type-dependent conformation of chromosome III, and also moderately reduces the selection of *HML* as a donor in *MAT α* cells (Szeto et al., 1997; Wu and Haber, 1996).

However, several considerations indicate that this cannot be the sole mechanism by which donor preference is regulated, and that an additional, more active mechanism must operate once a break is made at *MAT*. First, deletion of the minimal left part of RE prevents efficient selection of *HML* in *MAT α* cells

yet has no effect on the conformation of the chromosome in that mating type. Second, *MAT* interacts more frequently with *HMR*, in both mating types, yet it selects *HML* in *MAT α* cells. The high contact probability of *HMR* with *MAT* may be one reason that *HMR* is the default donor whenever switching with *HML* is impaired in *MAT α* cells. Combined these data indicate that the conformation of chromosome III prior to switching may contribute but is not sufficient to select the preferred donor.

We propose that the RE modulates chromosome conformation and left-arm usage during mating-type switching using distinct mechanisms. The right portion of the RE establishes mating-type-specific conformations prior to switching that set up the chromosome spatially such that in *MAT α* cells the left arm is sequestered away from *MAT* and therefore *HMR* outcompetes *HML* for interactions with *MAT*. In contrast, in *MAT α* cells the left arm explores space around the centromere-proximal domain up to the *MAT* locus, which may make *HML* more competitive for interactions with *MAT*. However, the competitive advantage of *HML* due to this spatial arrangement is not sufficient for exclusive selection of *HML*. To achieve higher donor selectivity, upon initiation of switching by induction of a DSB at *MAT*, the left portion of the RE actively engages with the *MAT* locus possibly through Fkh1p-mediated interaction with the DSB at *MAT* (Li et al., 2012). The pre-existing conformation of the left arm near *MAT* in *MAT α* cells may also contribute by facilitating this association. From these studies, we conclude that the RE is a composite element with the left portion playing a catalytic role in *MAT α* cells during switching and the right portion playing a structural role in both mating types that can help guide subsequent donor selection.

EXPERIMENTAL PROCEDURES

Hi-C and 5C analysis were performed as described before (Belton et al., 2012). Interaction data were binned at 10 or 30 kb and corrected for biases by the ICE method Imakaev et al., 2012) and then read normalized to facilitate comparison between data sets. 5C data were also normalized for genomic distance as described in Sanyal et al. (2012). Statistical differences between Hi-C data sets and 5C data sets were determined as described in the results and in the Supplemental Experimental Procedures. Live-cell imaging was performed as described by Lassadi et al. (2015), and the fraction of cells in which pairs of loci that were in close spatial proximity (distance <250 nm) was quantified. Yeast mutant were generated using standard techniques and grown in logarithmic phase for Hi-C/5C and live-cell-imaging analysis. Experimental details are provided in the Supplemental Experimental Procedures.

ACCESSION NUMBERS

Raw and processed 5C and Hi-C data as well as code for statistical analysis of the data are available at NCBI GEO under the accession number GSE73890.

SUPPLEMENTAL INFORMATION

Supplemental Information includes Supplemental Experimental Procedures, seven figures, and four tables and can be found with this article online at <http://dx.doi.org/10.1016/j.celrep.2015.10.063>.

AUTHOR CONTRIBUTIONS

J.-M.B. and J.D. designed the study. J.-M.B. performed the 5C and Hi-C experiments. S.A., S.C., I.L., I.G., and K.B. performed and analyzed imaging exper-

iments. J.-M.B., B.R.L., M.A.M.-R., and D.B. analyzed the data. J.-M.B., K.B., and J.D. wrote the paper. J.B., B.R.L., D.B., M.A.M.-R., and J.D. analyzed 5C data. J.B., M.A.M.-R., K.B., and J.D. wrote the manuscript.

ACKNOWLEDGMENTS

We acknowledge financial support from the National Human Genome Research Institute (HG003143) to J.D.; the Human Frontiers Science Program (RGP0044/2011) to J.D., K.B., and M.A.M.-R.; the Spanish MINECO (BFU2010-19310/BMC and BFU2013-47736-P) to M.A.M.-R.; and the French ANR (SVSE5 ANDY) to K.B. J.D. is an investigator of the Howard Hughes Medical Institute.

Received: May 25, 2015

Revised: August 27, 2015

Accepted: October 21, 2015

Published: November 19, 2015

REFERENCES

- Agmon, N., Liefshitz, B., Zimmer, C., Fabre, E., and Kupiec, M. (2013). Effect of nuclear architecture on the efficiency of double-strand break repair. *Nat. Cell Biol.* **15**, 694–699.
- Belton, J.-M., McCord, R.P., Gibcus, J.H., Naumova, N., Zhan, Y., and Dekker, J. (2012). Hi-C: a comprehensive technique to capture the conformation of genomes. *Methods* **58**, 268–276.
- Berger, A.B., Cabal, G.G., Fabre, E., Duong, T., Buc, H., Nehrbass, U., Olivo-Marin, J.-C., Gadal, O., and Zimmer, C. (2008). High-resolution statistical mapping reveals gene territories in live yeast. *Nat. Methods* **5**, 1031–1037.
- Bressan, D.A., Vazquez, J., and Haber, J.E. (2004). Mating type-dependent constraints on the mobility of the left arm of yeast chromosome III. *J. Cell Biol.* **164**, 361–371.
- Bystricky, K., Laroche, T., van Houwe, G., Blaszczyk, M., and Gasser, S.M. (2005). Chromosome looping in yeast: telomere pairing and coordinated movement reflect anchoring efficiency and territorial organization. *J. Cell Biol.* **168**, 375–387.
- Bystricky, K., Van Attikum, H., Montiel, M.-D., Dion, V., Gehlen, L., and Gasser, S.M. (2009). Regulation of nuclear positioning and dynamics of the silent mating type loci by the yeast Ku70/Ku80 complex. *Mol. Cell Biol.* **29**, 835–848.
- Dekker, J., Rippe, K., Dekker, M., and Kleckner, N. (2002). Capturing chromosome conformation. *Science* **295**, 1306–1311.
- Dekker, J., Marti-Renom, M.A., and Mirny, L.A. (2013). Exploring the three-dimensional organization of genomes: interpreting chromatin interaction data. *Nat. Rev. Genet.* **14**, 390–403.
- Dostie, J., Richmond, T.A., Anaout, R.A., Selzer, R.R., Lee, W.L., Honan, T.A., Rubio, E.D., Krumm, A., Lamb, J., Nusbaum, C., et al. (2006). Chromosome Conformation Capture Carbon Copy (5C): a massively parallel solution for mapping interactions between genomic elements. *Genome Res.* **16**, 1299–1309.
- Duan, Z., Andronescu, M., Schutz, K., McIlwain, S., Kim, Y.J., Lee, C., Shendure, J., Fields, S., Blau, C.A., and Noble, W.S. (2010). A three-dimensional model of the yeast genome. *Nature* **465**, 363–367.
- Gotta, M., Laroche, T., Formenton, A., Maillet, L., Scherthan, H., and Gasser, S.M. (1996). The clustering of telomeres and colocalization with Rap1, Sir3, and Sir4 proteins in wild-type *Saccharomyces cerevisiae*. *J. Cell Biol.* **134**, 1349–1363.
- Haber, J.E. (1998a). A locus control region regulates yeast recombination. *Trends Genet.* **14**, 317–321.
- Haber, J.E. (1998b). Mating-type gene switching in *Saccharomyces cerevisiae*. *Annu. Rev. Genet.* **32**, 561–599.
- Haber, J.E. (2012). Mating-type genes and MAT switching in *Saccharomyces cerevisiae*. *Genetics* **191**, 33–64.
- Hakim, O., Resch, W., Yamane, A., Klein, I., Kieffer-Kwon, K.-R., Jankovic, M., Oliveira, T., Bothmer, A., Voss, T.C., Ansarah-Sobrinho, C., et al. (2012). DNA

- damage defines sites of recurrent chromosomal translocations in B lymphocytes. *Nature* **484**, 69–74.
- Imakaev, M., Fudenberg, G., McCord, R.P., Naumova, N., Goloborodko, A., Lajoie, B.R., Dekker, J., and Mirny, L.A. (2012). Iterative correction of Hi-C data reveals hallmarks of chromosome organization. *Nat. Methods* **9**, 999–1003.
- Jin, Q., Trelles-Sticken, E., Scherthan, H., and Loidl, J. (1998). Yeast nuclei display prominent centromere clustering that is reduced in nondividing cells and in meiotic prophase. *J. Cell Biol.* **141**, 21–29.
- Jin, Q.W., Fuchs, J., and Loidl, J. (2000). Centromere clustering is a major determinant of yeast interphase nuclear organization. *J. Cell Sci.* **113**, 1903–1912.
- Lajoie, B.R., van Berkum, N.L., Sanyal, A., and Dekker, J. (2009). My5C: web tools for chromosome conformation capture studies. *Nat. Methods* **6**, 690–691.
- Lassadi, I., Kamgoué, A., Goiffon, I., Tanguy-le-Gac, N., and Bystricky, K. (2015). Differential chromosome conformations as hallmarks of cellular identity revealed by mathematical polymer modeling. *PLoS Comput. Biol.* **11**, e1004306.
- Li, J., Coïc, E., Lee, K., Lee, C.-S., Kim, J.-A., Wu, Q., and Haber, J.E. (2012). Regulation of budding yeast mating-type switching donor preference by the FHA domain of Fkh1. *PLoS Genet.* **8**, e1002630.
- Lieberman-Aiden, E., van Berkum, N.L., Williams, L., Imakaev, M., Ragozcy, T., Telling, A., Amit, I., Lajoie, B.R., Sabo, P.J., Dorschner, M.O., et al. (2009). Comprehensive mapping of long-range interactions reveals folding principles of the human genome. *Science* **326**, 289–293.
- Meaburn, K.J., Misteli, T., and Soutoglou, E. (2007). Spatial genome organization in the formation of chromosomal translocations. *Semin. Cancer Biol.* **17**, 80–90.
- Miele, A., Bystricky, K., and Dekker, J. (2009). Yeast silent mating type loci form heterochromatic clusters through silencer protein-dependent long-range interactions. *PLoS Genet.* **5**, e1000478.
- Naumova, N., Imakaev, M., Fudenberg, G., Zhan, Y., Lajoie, B.R., Mirny, L.A., and Dekker, J. (2013). Organization of the mitotic chromosome. *Science* **342**, 948–953.
- Roix, J.J., McQueen, P.G., Munson, P.J., Parada, L.A., and Misteli, T. (2003). Spatial proximity of translocation-prone gene loci in human lymphomas. *Nat. Genet.* **34**, 287–291.
- Rustchenko, E.P., Curran, T.M., and Sherman, F. (1993). Variations in the number of ribosomal DNA units in morphological mutants and normal strains of *Candida albicans* and in normal strains of *Saccharomyces cerevisiae*. *J. Bacteriol.* **175**, 7189–7199.
- Sanyal, A., Lajoie, B.R., Jain, G., and Dekker, J. (2012). The long-range interaction landscape of gene promoters. *Nature* **489**, 109–113.
- Simon, P., Houston, P., and Broach, J. (2002). Directional bias during mating type switching in *Saccharomyces* is independent of chromosomal architecture. *EMBO J.* **21**, 2282–2291.
- Sun, K., Coïc, E., Zhou, Z., Durrens, P., and Haber, J.E. (2002). *Saccharomyces* forkhead protein Fkh1 regulates donor preference during mating-type switching through the recombination enhancer. *Genes Dev.* **16**, 2085–2096.
- Szeto, L., and Broach, J.R. (1997). Role of alpha2 protein in donor locus selection during mating type interconversion. *Mol. Cell. Biol.* **17**, 751–759.
- Szeto, L., Fafalios, M.K., Zhong, H., Vershon, A.K., and Broach, J.R. (1997). Alpha2p controls donor preference during mating type interconversion in yeast by inactivating a recombinational enhancer of chromosome III. *Genes Dev.* **11**, 1899–1911.
- Therizols, P., Duong, T., Dujon, B., Zimmer, C., and Fabre, E. (2010). Chromosome arm length and nuclear constraints determine the dynamic relationship of yeast subtelomeres. *Proc. Natl. Acad. Sci. USA* **107**, 2025–2030.
- Tjong, H., Gong, K., Chen, L., and Alber, F. (2012). Physical tethering and volume exclusion determine higher-order genome organization in budding yeast. *Genome Res.* **22**, 1295–1305.
- Trelles-Sticken, E., Dresser, M.E., and Scherthan, H. (2000). Meiotic telomere protein Ndj1p is required for meiosis-specific telomere distribution, bouquet formation and efficient homologue pairing. *J. Cell Biol.* **151**, 95–106.
- Weiss, K., and Simpson, R.T. (1997). Cell type-specific chromatin organization of the region that governs directionality of yeast mating type switching. *EMBO J.* **16**, 4352–4360.
- Wu, X., and Haber, J.E. (1995). MATa donor preference in yeast mating-type switching: activation of a large chromosomal region for recombination. *Genes Dev.* **9**, 1922–1932.
- Wu, X., and Haber, J.E. (1996). A 700 bp cis-acting region controls mating-type dependent recombination along the entire left arm of yeast chromosome III. *Cell* **87**, 277–285.
- Wu, X., Wu, C., and Haber, J.E. (1997). Rules of donor preference in *saccharomyces* mating-type gene switching revealed by a competition assay involving two types of recombination. *Genetics* **147**, 399–407.
- Wu, C., Weiss, K., Yang, C., Harris, M.A., Tye, B.-K., Newlon, C.S., Simpson, R.T., and Haber, J.E. (1998a). Mcm1 regulates donor preference controlled by the recombination enhancer in *Saccharomyces* mating-type switching. *Genes Dev.* **12**, 1726–1737.
- Zhang, Y., McCord, R.P., Ho, Y.J., Lajoie, B.R., Hildebrand, D.G., Simon, A.C., Becker, M.S., Alt, F.W., and Dekker, J. (2012). Spatial organization of the mouse genome and its role in recurrent chromosomal translocations. *Cell* **148**, 908–921.
- Zimmer, C., and Fabre, E. (2011). Principles of chromosomal organization: lessons from yeast. *J. Cell Biol.* **192**, 723–733.